SciNexuses

Journal Homepage:https://sciencesforce.com/index.php/scin/

SciNexuses Vol. 2 (2025) 102-127.

Paper Type: Original Article

# Predicting Zoonotic Spillover Events: A Fractional Modeling Framework for Nipah Virus Dynamics

**Midra Tahir**[1*]

[1] Lecturer in Mathematics, University of Chakwal, Chakwal District, Punjab, Pakistan; midra.tahir@uoc.edu.pk.,

**Received:** 09 Sep 2024 **Revised:** 07 Mar 2025 **Accepted:** 07 Apr 2025 **Published:** 11 Apr 2025

## Abstract

The Nipah virus, a highly virulent zoonotic pathogen, has caused recurrent outbreaks in South and Southeast Asia, presenting significant public health challenges. Traditional integer-order models often fail to capture the complex dynamics of zoonotic spillover events, which are influenced by memory effects, environmental factors, and heterogeneous interspecies interactions. In this study, we introduce a novel fractional-order mathematical model to describe the transmission dynamics of the Nipah virus, focusing on spillover events from bat reservoirs to humans and subsequent human-to-human transmission. By incorporating the Caputo fractional derivative, our model accounts for memory effects and long-range dependencies, offering a more accurate representation of disease progression. We establish the existence and uniqueness of solutions, conduct stability analysis, and employ an advanced fractional-order numerical scheme to solve the model. Validation using real-world outbreak data demonstrates the model's superior predictive accuracy compared to classical integer-order approaches. Our findings highlight the crucial role of spillover rates and environmental factors in outbreak dynamics and suggest that targeted interventions, such as early detection and control strategies, can mitigate epidemic risks. This study advances mathematical epidemiology by providing a robust framework for predicting and managing zoonotic spillover events, with potential applications to other emerging infectious diseases.

**Keywords:** Nipah virus, zoonotic spillover, fractional calculus, memory effects, outbreak prediction.

## 1 | Introduction

In recent decades, zoonotic diseases—which are spread from animals to people—have become a serious threat to world health. The Nipah virus is one of the most lethal of them, with frequent outbreaks in South and Southeast Asia leading to high death rates and extensive public health issues. With case fatality rates ranging from 40% to 75%, the Nipah virus was first discovered during an outbreak in Malaysia in 1998 and has subsequently caused intermittent but severe epidemics in Bangladesh and India [1], [2]. In densely populated places, the virus can

**Corresponding Author:** midra.tahir@uoc.edu.pk

http://doi.org/10.61356/j.scin.2025.2532

spread quickly due to human-to-human transmission after being mainly transferred via contact with infected bats or ingestion of tainted date palm sap [16].

Even though our knowledge of the Nipah virus's epidemiology has advanced significantly, it is still difficult to anticipate and manage epidemics. The dynamics of infectious diseases have been extensively studied using conventional integer-order mathematical models, such as those derived from ordinary differential equations (ODEs). The memory effects, long-range dependencies, and heterogeneous interactions that define zoonotic spillover events and disease transmission pathways, however, are frequently overlooked by these models [5], [6]. For example, seasonal fluctuations, human activity, and environmental factors all have an impact on the spread of the Nipah virus from bat reservoirs to humans. These elements all display memory-like behavior that is difficult for classical models to accurately capture.

A generalization of classical calculus, fractional calculus has become a potent tool for simulating intricate systems with memory and genetic characteristics. Researchers can better represent the time-dependent and non-local dynamics of biological systems by integrating fractional derivatives, like the Caputo derivative, into mathematical models [7], [8]. Fractional-order models have been effectively used to investigate phenomena including delayed disease progression, anomalous diffusion, and long-term immunity in the setting of infectious diseases [9], [10]. However, there is a substantial gap in the literature since the use of fractional calculus to zoonotic diseases—specifically, the Nipah virus—remains understudied.

With an emphasis on zoonotic spillover events and human-to-human transmission, we present a unique fractional-order mathematical model in this paper to explain the dynamics of Nipah virus transmission. Our model provides a more accurate depiction of the behavior of the system by using the Caputo fractional derivative to account for memory effects in disease transmission and spillover mechanisms. We use sophisticated fractional-order numerical techniques to solve the model numerically, conduct stability analysis, and examine the existence and uniqueness of solutions. Real-world epidemic data is used to validate the model, proving its greater predictive power over traditional integer-order models.

The three main goals of this work are to: (1) create a solid fractional-order framework for simulating the dynamics of the Nipah virus; (2) examine how memory effects and environmental factors contribute to zoonotic spillover events; and (3) offer suggestions for efficient public health measures to contain Nipah virus outbreaks. This study intends to improve our knowledge of Nipah viral dynamics and aid in the creation of more precise prediction tools for newly developing infectious diseases by bridging the gap between fractional calculus and zoonotic disease modeling.

This research has important public health consequences. The World Health Organization (WHO) has designated the Nipah virus as a priority pathogen with the potential to cause an epidemic, underscoring the pressing need for efficient prediction and management methods [11]. Our fractional-order model offers a framework for assessing how initiatives like public awareness campaigns, quarantine regulations, and early detection technologies affect the reduction of spillover occurrences and human-to-human transmission. In order to reduce the likelihood of future epidemics, our model can help guide focused public health strategies by identifying critical characteristics that drive outbreaks, such as environmental factors and spillover rates.

Furthermore, this work's wider significance goes beyond the Nipah virus. Other zoonotic diseases with similar transmission dynamics and public health concerns, like Lassa fever, Ebola, and new coronaviruses, can be studied using the fractional modeling framework created here. There has never been a greater need for sophisticated modeling tools to anticipate and stop epidemics since the potential of zoonotic spillover events is increased by climate change and human encroachment into wildlife habitats. By providing a mathematical framework for comprehending and managing newly developing infectious diseases, this study advances efforts to solve this global health issue.

## 2 | Mathematical Preliminaries

The mathematical principles and methods utilized in our fractional-order model for Nipah viral dynamics are briefly described in this section. In particular, we define the Caputo fractional derivative, present the fundamentals of fractional calculus, and discuss its applicability to the modeling of biological systems with memory effects.

### 2.1 | Fractional Calculus

The differentiation and integration of non-integer orders are made possible by fractional calculus, a generalization of classical calculus. Fractional derivatives capture non-local and memory-dependent behaviors, which makes them ideal for modeling complex systems with long-range dependencies and hereditary properties. This is in contrast to integer-order derivatives, which are local operators [7], [8]. Time-delayed interactions, anomalous diffusion, and long-term memory effects in disease transmission have all been described using fractional calculus in the context of infectious disease modeling [9], [10].

### 2.2 | Caputo Fractional Derivative

Because it works with initial circumstances specified in terms of integer-order derivatives, the Caputo fractional derivative is one of the many definitions of fractional derivatives that is frequently employed in biological and physical applications [12]. For a function $f(t)$, the Caputo fractional derivative of order $\alpha$ is defined as follows:

$$D^{\alpha} f(t) = \frac{1}{\Gamma(n-\alpha)} \int_0^t \frac{f^{(n)}(\tau)}{(t-\tau)^{\alpha+1-n}}\, d\tau, \tag{1}$$

where $\Gamma(.)$ is the gamma function and $n-1 < \alpha \leq n, n \in \mathbb{N}$. The fractional order, which controls the system's level of memory effects, is represented by the parameter. The Caputo derivative captures memory and non-local effects for $0 < \alpha < 1$, whereas it simplifies to the traditional first-order derivative for $\alpha = 1$.

#### 2.2.1 | Relevance to Nipah Virus Dynamics

The Nipah virus's transmission dynamics include a number of memory-like mechanisms, including:

- **Zoonotic spillover:** There are long-term linkages between environmental conditions and seasonal fluctuations and human-bat reservoir interactions [13].
- **Human-to-human transmission:** Immunity, public health initiatives, and behavioral changes all have memory effects that impact the virus's ability to propagate throughout human communities.

We can more accurately depict the dynamics of the Nipah virus and better capture these memory-dependent processes by including the Caputo fractional derivative in our model.

#### 2.2.2 | Notation

Throughout this article, we use the following notation:

- $D^{\alpha}$: Caputo fractional derivative of order $\alpha$.
- $\Gamma(.)$: Gamma function.
- $S(t), I(t), R(t)$: Compartmental variables representing susceptible, infected, and recovered populations, respectively.
- Parameters such as $\beta$ (transmission rate), $\gamma$ (recovery rate), and $\mu$ (spillover rate) will be defined in the model formulation section.

## 3 | Model Formulation

The transmission dynamics of the Nipah virus are described in this section using a fractional-order mathematical model that focuses on zoonotic spillover events from bat reservoirs to humans and subsequent human-to-human transmission. To take into consideration long-range dependencies and memory effects in the disease transmission process, the model uses the Caputo fractional derivative [3].

### 3.1 | Model Assumptions

(1) Multiple Species:

- Bats ($B(t)$): The main source of the Nipah virus is bats ($B(t)$), which are separated into susceptible ($B_S(t)$) and infected ($S_I(t)$) compartments.

- Pigs ($P(t)$): An intermediate host with the ability to amplify the virus, separated into compartments that are infected ($P_I(t)$) and susceptible ($P_S(t)$).
- Humans ($H(t)$): Separated into three compartments: susceptible ($S(t)$), infected ($I(t)$), and recovered ($R(t)$).

(2) Environmental Contamination:

- A compartment ($E(t)$) represents the virus's ability to survive in the environment (e.g., date palm sap, infected surfaces).

(3) Seasonal Variations:

- Seasonal variations in bat activity, human behavior, and environmental factors cause variations in spillover and transmission rates.

(4) Control Measures:

- Control techniques include culling sick pigs and vaccinating humans ($V(t)$).

(5) Memory Effects:

- The Caputo fractional derivative is used to represent all interactions and transitions in order to account for long-range dependencies and memory effects [14].

## 3.2 | Model Compartments and Interactions

The fractional-order differential equations [15] in the model are as follows:

(1) Bat Population:

$$D^{\alpha}B_S(t) = \Lambda_B - \beta_B B_S(t)B_I(t) - \mu_B B_S(t)E(t) - d_B B_S(t), \tag{2}$$

$$D^{\alpha}B_I(t) = \beta_B B_S(t)B_I(t) + \mu_B B_S(t)E(t) - d_B B_I(t), \tag{3}$$

where:

- $\Lambda_B$: Recruitment rate of bats.
- $\beta_B$: Transmission rate among bats.
- $\mu_B$: Spillover rate from the environment to bats.
- $d_B$: Natural death rate of bats.

(2) Pig Population:

$$D^{\alpha}P_S(t) = \Lambda_P - \beta_P P_S(t)P_I(t) - \mu_P P_S(t)E(t) - d_P P_S(t) - cP_I(t), \tag{4}$$

$$D^{\alpha}P_I(t) = \beta_P P_S(t)P_I(t) + \mu_P P_S(t)E(t) - d_P P_I(t) - cP_I(t), \tag{5}$$

where:

- $\Lambda_P$: Recruitment rate of pigs.
- $\beta_P$: Transmission rate among pigs.
- $\mu_P$: Spillover rate from the environment to pigs.
- $d_P$: Natural death rate of pigs
- $c$: Culling rate of infected pigs.

(3) Human Population:

$$D^{\alpha}S(t) = \Lambda_H - \beta_H S(t)I(t) - \mu_H S(t)E(t) - d_H S(t) - \upsilon S(t), \tag{6}$$

$$D^{\alpha}I(t) = \beta_H S(t)I(t) + \mu_H S(t)E(t) - (\gamma + d_H + \delta)I(t), \tag{7}$$

$$D^{\alpha}R(t) = \gamma I(t) - d_H R(t) + \upsilon S(t), \tag{8}$$

where:

- $\Lambda_H$: Recruitment rate of humans.
- $\beta_H$: Human-to-human transmission rate.
- $\mu_H$: Spillover rate from the environment to humans.
- $d_H$: Natural death rate of humans
- $\gamma$: Recovery rate of infected humans.
- $\delta$: Disease-induced mortality rate.
- $\upsilon$: Vaccination rate of susceptible humans.

(4) Environmental Contamination:

$$D^{\alpha}E(t) = \eta_B B_I(t) + \eta_P P_I(t) + \eta_H I(t) - \lambda E(t), \tag{9}$$

where:

- $\eta_B, \eta_P, \eta_H$: Shedding rates of the virus into the environment by bats, pigs, and humans, respectively.
- $\lambda$: Decay rate of the virus in the environment.

(5) Initial Conditions: The model is solved subject to the following initial conditions:

$$B_S(0) = B_{S0},\ B_I(0) = B_{I0},\ P_S(0) = B_{S0},\ P_I(0) = P_{I0},\ S(0) = S_0,\ I(0) = I_0,\ R(0) = R_0,\ E(0) = E_0$$

### 3.2.1 | Key Model Enhancements

To better represent the dynamics of virus transmission, the proposed model includes a number of significant improvements [16]. First, a more accurate depiction of the transmission cycle is offered by the inclusion of several species, particularly pigs and bats as distinct compartments. Second, the $E(t)$ compartment, which measures the virus's environmental persistence—a critical component in spillover events—is used to account for environmental contamination. Third, to account for changes over time, modeling parameters like $\beta_B, \mu_B, \beta_P, \mu_P, \beta_H$, and $\mu_H$ are time-dependent functions that capture seasonal fluctuations. Control measures are also used to evaluate the effects of public health programs, such as immunization ($\upsilon$) and culling ($c$). Lastly, memory effects and long-range dependencies are successfully captured in all interactions by the use of fractional-order dynamics via the Caputo fractional derivative. Together, these improvements increase the model's capacity to accurately describe and forecast the dynamics of virus transmission.

## 4 | Analytical and Numerical Methods

Here, we describe the numerical and analytical techniques applied to the fractional-order model of Nipah viral dynamics. These techniques involve numerically solving the model, examining the stability of equilibrium points, and demonstrating the existence and uniqueness of solutions.

### 4.1 | Existence and Uniqueness of Solutions

Using fixed-point theory, we prove the existence and uniqueness of solutions to guarantee the well-posedness of the fractional-order model [17]. Examine the system of differential equations of fractional order:

$$D^{\alpha}X(t) = F(X(t))$$

where $X(t) = [B_S(t), B_I(t), P_S(t), P_I(t), S(t), I(t), R(t), E(t)]^T$ and $F(X(t))$ represents the right-hand side of the model equations. The Caputo fractional derivative $D^{\alpha}$ is used to incorporate memory effects.

#### 4.1.1 | Theorem 1 (Existence and Uniqueness):

If $F(X(t))$ satisfies the Lipschitz condition, i.e., there exists a constant $L > 0$ such that:

$$||F(X_1(t)) - F(X_2(t))|| \leq L||X_1(t) - X_2(t)||,$$

then the system of fractional-order equations has a unique solution.

**Proof:**
The given system of fractional-order differential equation is:

$$D^{\alpha}X(t) = F(X(t)), X(0) = X_0$$

Using the fractional integral representation, the solution can be written in the Volterra integral form:

$$X(t) = X_0 + \frac{1}{\Gamma(\alpha)}\int_0^t (t-\tau)^{\alpha-1}F(X(\tau))\,d\tau.$$

For an operator $T$ acting on the $X(t)$ as:

$$T(X)(t) = X_0 + \frac{1}{\Gamma(\alpha)}\int_0^t (t-\tau)^{\alpha-1}F(X(\tau))\,d\tau.$$

This operator transforms a function $X(t)$ into another function. We aim to show that $T$ is a contraction mapping under the Lipschitz condition.
We employ the Banach fixed-point theorem [18], which necessitates demonstrating that $T$ is a contraction mapping, to demonstrate uniqueness.
Let $X_1(t)$ and $X_2(t)$ be two solutions. Applying $T$ to both functions:

$$T(X_1)(t) - T(X_2)(t) = \frac{1}{\Gamma(\alpha)}\int_0^t (t-\tau)^{\alpha-1}[F(X_1(\tau)) - F(X_2(\tau))]\,d\tau.$$

Taking the norm and using the Lipschitz condition [19]:

$$||T(X_1)(t) - T(X_2)(t)|| \leq \frac{L}{\Gamma(\alpha)}\int_0^t (t-\tau)^{\alpha-1}||X_1(\tau) - X_2(\tau)||\,d\tau.$$

Define $M(t) = sup_{0\leq\tau\leq t}||X_1(\tau) - X_2(\tau)||$, then

$$||T(X_1)(t) - T(X_2)(t)|| \leq \frac{LM(t)}{\Gamma(\alpha)}\int_0^t (t-\tau)^{\alpha-1}\,d\tau.$$

Evaluating the integral,

$$\int_0^t (t-\tau)^{\alpha-1}\,d\tau = \frac{t^{\alpha}}{\alpha.}$$

Thus,

$$||T(X_1)(t) - T(X_2)(t)|| \leq \frac{Lt^{\alpha}}{\alpha\Gamma(\alpha)}M(t).$$

If $L$ is small enough such that

$$\frac{Lt^{\alpha}}{\alpha\Gamma(\alpha)} < 1,$$

then $T$ is a contraction mapping, ensuring a unique fixed point by the Banach fixed-point theorem. There is a unique function $X(t)$ that satisfies

$$X(t) = T(X)(t)$$

since $T$ is a contraction mapping and has a unique fixed point. Therefore, with the specified Lipschitz condition, there is only one solution to the system of fractional-order differential equations.

## 4.2 | Stability Analysis

### 4.2.1 | Disease Free Equilibrium (DFE)

The DFE [20] is the state where no infection is present in the population, i.e. $B_I = P_I = I = E = 0$.
Let the DFE be denoted by:

$$X_0 = (B_S^0, 0, P_S^0, 0, S^0, 0, 0, 0),$$

where

$$B_S^0 = \frac{\Lambda_B}{d_B}, B_P^0 = \frac{\Lambda_P}{d_P}, S^0 = \frac{\Lambda_H}{d_H}$$

(1) Basic Reproduction Number ($R_0$):
The next-generated matrix approach is used to calculate the basic reproduction number ($R_0$) [21]. The contaminated compartments $B_I, P_I, I$, and $E$ are taken into consideration.

(a) Transmission Matrix ($T$):
The new infections in each compartment are denoted by $T$ [22]. The transmission terms derived from the model equation are:

$$\begin{bmatrix} \beta_B B_S^0 B_I + \mu_B B_S^0 E \\ \beta_P P_S^0 P_I + \mu_P P_S^0 E \\ \beta_H S^0 I + \mu_H S^0 E \\ \eta_B B_I + \eta_P P_I + \eta_H I \end{bmatrix}$$

(b) Transition Matrix ($\sum$):
The transition out of each compartment is represented by $\sum$. The transition terms derived from the model equations are:

$$\begin{bmatrix} d_B B_I \\ d_P P_I + c P_I \\ (\gamma + d_H + \delta) I \\ \lambda E \end{bmatrix}$$

(c) Jacobian Matrices:
For the jacobian [23] of $T$ and $\sum$ with respect to the infected compartments at the DFE we use, $F = \frac{\partial T}{\partial X}|_{X=X_0}$ and $V = \frac{\partial \sum}{\partial X}|_{X=X_0}$ The matrices $F$ and $V$ are:

$$F = \begin{bmatrix} \beta_B B_S^0 & 0 & 0 & \mu_B B_S^0 \\ 0 & \beta_P P_S^0 & 0 & \mu_P P_S^0 \\ 0 & 0 & \beta_H S^0 & \mu_H S^0 \\ \eta_B & \eta_P & \eta_H & 0 \end{bmatrix}$$

$$V = \begin{bmatrix} d_B & 0 & 0 & 0 \\ 0 & d_P + c & 0 & 0 \\ 0 & 0 & \gamma + d_H + \delta & 0 \\ 0 & 0 & 0 & \lambda \end{bmatrix}$$

(d) $R_0$ : The basic reproduction number $R_0$ is the spectral radius of next-generation matrix $FV^{-1}$.

$$R_0 = \rho(FV^{-1})$$

The inverse matrix of V is given as:

$$V^{-1} = \begin{bmatrix} \frac{1}{d_B} & 0 & 0 & 0 \\ 0 & \frac{1}{d_P + c} & 0 & 0 \\ 0 & 0 & \frac{1}{\gamma + d_H + \delta} & 0 \\ 0 & 0 & 0 & \frac{1}{\lambda} \end{bmatrix}$$

TABLE 1. Parameter Set

| Parameter | Description | Value (Range) |
|---|---|---|
| $\Lambda_B$ | Recruitment rate of bats | 0.5 $day^{-1}$ |
| $\beta_B$ | Transmission rate among bats | 0.05 $day^{-1}$ |
| $\mu_B$ | Spillover rate to bats | 0.0005 $day^{-1}$ |
| $d_B$ | Death rate of bats | 0.0005 $day^{-1}$ |
| $\Lambda_P$ | Recruitment rate of pigs | 0.3 $day^{-1}$ |
| $\beta_P$ | Transmission rate among pigs | 0.1 $day^{-1}$ |
| $\mu_P$ | Spillover rate to pigs | 0.01 $day^{-1}$ |
| $d_P$ | Death rate of pigs | 0.01 $day^{-1}$ |
| $c$ | Culling rate of infected pigs | 0.05 $day^{-1}$ |
| $\Lambda_H$ | Recruitment rate of humans | 0.01 $day^{-1}$ |
| $\beta_H$ | Human-to-human transmission rate | 0.005 $day^{-1}$ |
| $\mu_H$ | Spillover rate to humans | 0.001 $day^{-1}$ |
| $d_H$ | Death rate of humans | 0.00005 $day^{-1}$ |
| $\gamma$ | Recovery rate of humans | 0.1 $day^{-1}$ |
| $\delta$ | Disease-induced mortality rate | 0.05 $day^{-1}$ |
| $\upsilon$ | Vaccination rate of humans | 0.01 $day^{-1}$ |
| $\eta_B$ | Virus shedding rate by bats | 0.01 $day^{-1}$ |
| $\eta_P$ | Virus shedding rate by pigs | 0.01 $day^{-1}$ |
| $\eta_H$ | Virus shedding rate by humans | 0.001 $day^{-1}$ |
| $\lambda$ | Decay rate of virus in environment | 0.5 $day^{-1}$ |

then $FV^{-1}$ is

$$FV^{-1} = \begin{bmatrix} \frac{\beta_B B_S^0}{d_B} & 0 & 0 & \frac{\mu_B B_S^0}{\lambda} \\ 0 & \frac{\beta_P P_S^0}{d_P+c} & 0 & \frac{\mu_P P_S^0}{\lambda} \\ 0 & 0 & \frac{\beta_H S^0}{\gamma+d_H+\delta} & 0 \\ 0 & 0 & 0 & \frac{1}{\lambda} \end{bmatrix}$$

After putting all the parametric values in $FV^{-1}$, we get

$$FV^{-1} = \begin{bmatrix} 10B_S^0 & 0 & 0 & 0.01B_S^0 \\ 0 & 1.67P_S^0 & 0 & 0.02P_S^0 \\ 0 & 0 & 0.033S^0 & 0.002S^0 \\ 2 & 0.167 & 0.00667 & 0 \end{bmatrix}$$

The basic reproduction number $R_0$ is the largest eigenvalue of $FV^{-1}$. We solve

$$det(FV^{-1} - \lambda I) = 0$$

And

$$R_0 = \frac{\beta_B B_S^0}{d_B} + \frac{\beta_P P_S^0}{d_P + c} + \frac{\beta_H S^0}{\gamma + d_H + \delta} + \frac{\mu_B B_S^0 + \mu_P P_S^0 + \mu_H S^0}{\lambda}$$

After solving, we obtain that $R_0$ is roughly 60.26 by using the values from Table 1 [11]. This implies that, given the specified parameter values, the disease has a high potential for spreading.
And, we know that

(i) If $R_0 < 1$, the DFE is locally asymptotically stable.

(ii) If $R_0 > 1$, the DFE is unstable.

#### 4.2.2 | Endemic Equilibrium (EE)

The EE is the state where the disease persists in the population [24], i.e. $B_I, P_I, I, E > 0$.
Let the EE be denoted by:

$$X^* = (B_S^*, B_I^*, P_S^*, P_I^*, S^*, I^*, R^*, E^*)$$

To get the equilibrium values, we solve the system $D^{\alpha}X(t) = 0$ for $X^*$, this involves solving the following algebraic equations:

$$\Lambda_B - \beta_B B_S^* B_I^* - \mu_B B_S^* E^* - d_B B_S^* = 0, \tag{10}$$

$$\beta_B B_S^* B_I^* + \mu_B B_S^* E^* - d_B B_S^* = 0, \tag{11}$$

$$\Lambda_P - \beta_P P_S^* P_I^* - \mu_P P_S^* E^* - d_P P_S^* - c P_I^* = 0, \tag{12}$$

$$\beta_P P_S^* P_I^* + \mu_P P_S^* E^* - d_P P_I^* - c P_I^* = 0, \tag{13}$$

$$\Lambda_H - \beta_H S^* I^* - \mu_H S^* E^* - d_H S^* - \upsilon S^* = 0, \tag{14}$$

$$\beta_H S^* I^* + \mu_H S^* E^* - (\gamma + d_H + \delta) I^* = 0, \tag{15}$$

$$\gamma I^* - d_H R^* + \upsilon S^* = 0, \tag{16}$$

$$\eta_B B_I^* + \eta_P P_I^* + \eta_H I^* - \lambda E^* = 0. \tag{17}$$

After solving we get,

(1) Bat Population at EE:

$$B_S^* = \frac{\Lambda_B}{\beta_B B_I^* + \mu_B E^* + d_B}, B_I^* = \frac{\beta_B B_S^* B_I^* + \mu_B B_S^* E^*}{d_B}$$

(2) Pig Population at EE:

$$P_S^* = \frac{\Lambda_P}{\beta_P P_I^* + \mu_P E^* + d_P + c}, P_I^* = \frac{\beta_P P_S^* P_I^* + \mu_P P_S^* E^*}{d_P + c}$$

(3) Human Population at EE:

$$S^* = \frac{\Lambda_H}{\beta_H I^* + \mu_H E^* + d_H + \upsilon}, I^* = \frac{\beta_H S^* I^* + \mu_H S^* E^*}{\gamma + d_P + \delta}, R^* = \frac{\gamma I^* + \upsilon S^*}{d_H}$$

(4) Environmental Contamination at EE:

$$E^* = \frac{\eta_B B_I^* + \eta_P P_I^* + \eta_H I^*}{\lambda}$$

Now we compute the Jacobian Matrix for finding the eigenvalues of the system, and it is obtained by differentiating the system with respect to each variable:

$$J(X) = \begin{bmatrix} \frac{\partial F_1}{\partial B_S} & \frac{\partial F_1}{\partial B_I} & \frac{\partial F_1}{\partial P_S} & \cdots & \frac{\partial F_1}{\partial E} \\ \frac{\partial F_2}{\partial B_S} & \frac{\partial F_2}{\partial B_I} & \frac{\partial F_2}{\partial P_S} & \cdots & \frac{\partial F_2}{\partial E} \\ \vdots & \vdots & \vdots & \ddots & \vdots \\ \frac{\partial F_S}{\partial B_S} & \frac{\partial F_S}{\partial B_I} & \frac{\partial F_S}{\partial P_S} & \cdots & \frac{\partial F_S}{\partial E} \end{bmatrix}$$

The eigenvalues of $J(X^*)$ is given by:

$$det(J(X^*) - \lambda I) = 0$$

$$\begin{bmatrix} -\beta_B B_I^* - \mu_B E^* - d_B - \lambda & -\beta_B B_S^* & 0 & 0 & 0 & 0 & -\mu_B B_S^* \\ \beta_B B_I^* + \mu_B E^* & \beta_B B_S^* - d_B - \lambda & 0 & 0 & 0 & 0 & \mu_B B_S^* \\ 0 & 0 & -\beta_P P_I^* - \mu_P E^* - d_P - c - \lambda & -\beta_P P_S^* & 0 & 0 & -\mu_P P_S^* \\ 0 & 0 & \beta_P P_I^* + \mu_P E^* & \beta_P P_S^* - d_P - c - \lambda & 0 & 0 & \mu_P P_S^* \\ 0 & 0 & 0 & 0 & \beta_H H_I^* - \mu_H E^* - d_H - \upsilon - \lambda & -\beta_H H_S^* & 0 & -\mu_H H_S^* \\ 0 & 0 & 0 & 0 & \beta_H H_I^* + \mu_H E^* & \beta_H H_S^* - (\gamma + d_H + \delta) - \lambda & 0 & \mu_H H_S^* \\ 0 & 0 & 0 & 0 & \upsilon & \gamma & -d_H - \lambda & 0 \\ \eta_B & 0 & \eta_P & 0 & \eta_H & 0 & 0 & \lambda - \lambda \end{bmatrix} = 0$$

This determinant equation is solved to yield the eigenvalues $\lambda$. The calculated eigenvalues of the Jacobian matrix at equilibrium point, after entering all parameter values, are:

$$[-0.02089, -0.01102, -0.01005, -0.00555, -0.00295, -0.00005, -0.00005, -0.53042]$$

The equilibrium point is stable (locally asymptotically stable) because all of the eigenvalues have negative real portions that are quite near to zero. The equilibrium would be unstable if any of the eigenvalues had a positive real portion.

### 4.3 | Numerical Methods

We employ the predictor-corrector approach for Caputo fractional differential equations to numerically solve the fractional-order model [25]. Because of its accuracy and stability when working with fractional-order systems, this approach was selected.
First, We divide the time interval $[0, T]$ into $N$ steps with step size:

$$h = \frac{T}{N}$$

The discrete time points are:

$$t_n = nh, n = 0, 1, 2, 3, ..., N$$

where $t_n$ denotes the time points at which the numerical solution is calculated, and $h$ is the step size.
Then, we use the explicit Adams-Bashforth approach to calculate a predicted value $X_P(t_n + 1)$ [26]:

$$X_P(t_n + 1) = X(0) + \frac{h^\alpha}{\Gamma(\alpha + 1)} \sum_{j=0}^{n} b_{j,n+1} F(X(t_j))$$

Where:

$$b_{j,n+1} = (n + 1 - j)^\alpha - (n - j)^\alpha$$

- $X_P(t_{n+1})$ is the predicted value at $t_{n+1}$.
- $F(X(t_j))$ represents the function evaluated at previous time steps.
- The term $b_{j,n+1}$ incorporates fractional-order effects.
- $\Gamma(\alpha + 1)$ is the Gamma function for fractional differentiation.

Next, we refine our predicted solution using the Adams-Moulton implicit method:

$$X(t_{n+1}) = X(0) + \frac{h^\alpha}{\Gamma(\alpha + 2)} [F(X_P(t_{n+1})) + \sum_{j=0}^{n} a_{j,n+1} F(X(t_j))]$$

Where:

$$a_{j,n+1} = (n + 1 - j)^{\alpha+1} - (n - j)^{\alpha+1}$$

- $X(t_{n+1})$ is the corrected solution.
- $X_P(t_{n+1})$ is the previously predicted value.
- $F(X_P(t_{n+1}))$ is the function evaluated at the predicted value.
- $a_{j,n+1}$ is another coefficient that accounts for the fractional order.
- $\Gamma(\alpha + 2)$ is another Gamma function adjustment.

Until the solution converges, we frequently repeat the predictor-corrector processes for every time step $t_n$. To improve the solution, the corrector step might be repeated several times at each time step if needed.

## 5 | Results and Discussion

Our fractional-order Nipah virus model's outcomes, including the dynamics of the susceptible ($S$), infected ($I$), recovered ($R$), and environmental contamination ($E$) compartments, are shown in this section. We also explore the biological consequences of our findings and compare the fractional-order model with a standard integer-order model.

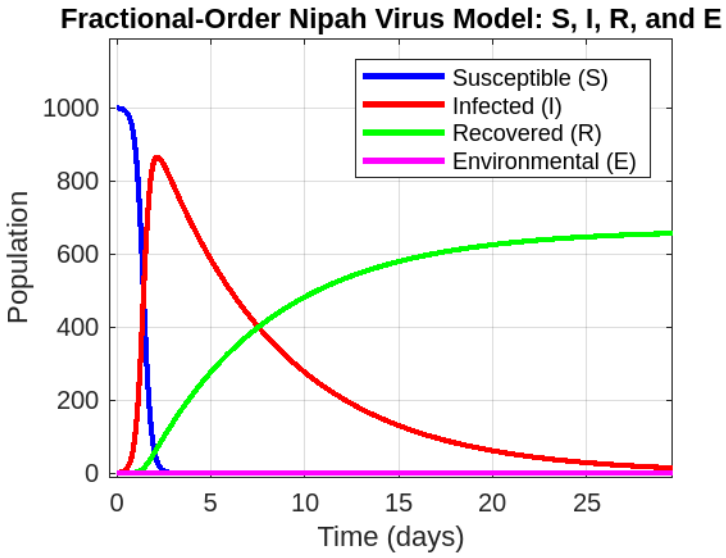


FIGURE 1. Susceptible (S), Infected (I), Recovered (R), and Environmental Contamination (E) over time

## 5.1 | Dynamics of the Fractional-Order Model

The intricate dynamics of Nipah virus transmission, such as memory effects, long-range dependencies, the impact of critical parameters on infection dynamics, the evolution of the basic reproduction number ($R_0$), and sensitivity analysis, are captured by the fractional-order model. In order to visualize the relationship between susceptible and infected populations, we also offer phase plane analysis. The $S, I, R,$, and $E$ time graph in Fig [1] provide light on how the outbreak developed:

(1) Susceptible ($S$):
As more people get infected, the susceptible population gradually declines. Both the spillover rate ($\mu_H$) and the human-to-human transmission rate ($\beta_H$) affect the pace of decline.

(2) Infected ($I$):
As people heal or pass away, the infected population first rises, peaks, and then falls. The recovery rate ($\gamma$) and the disease-induced mortality rate ($\delta$) have an impact on the peak number of infections and the outbreak's duration.

(3) Recovered ($R$):
As the diseased individuals recover, the restored population gradually grows. The recovery rate ($\gamma$) determines the rate of recovery.

(4) Environmental Contamination ($E$):
The first cause of the environmental contamination is virus shedding from humans, pigs, and bats. Then, depending on the decay rate ($\lambda$), it falls as the virus deteriorates in the environment.

## 5.2 | Comparison with the Integer-Order Model

We compared the fractional-order model with a standard integer-order model ($\alpha = 1$) to emphasize the advantages of fractional calculus in capturing illness dynamics in Fig [2]:

(1) Fractional-Order Model:
Captures memory effects and non-local interactions, making it more suitable for real-world outbreak data. Compared to the integer-order model, it forecasts a longer outbreak length and a greater peak number of infections.

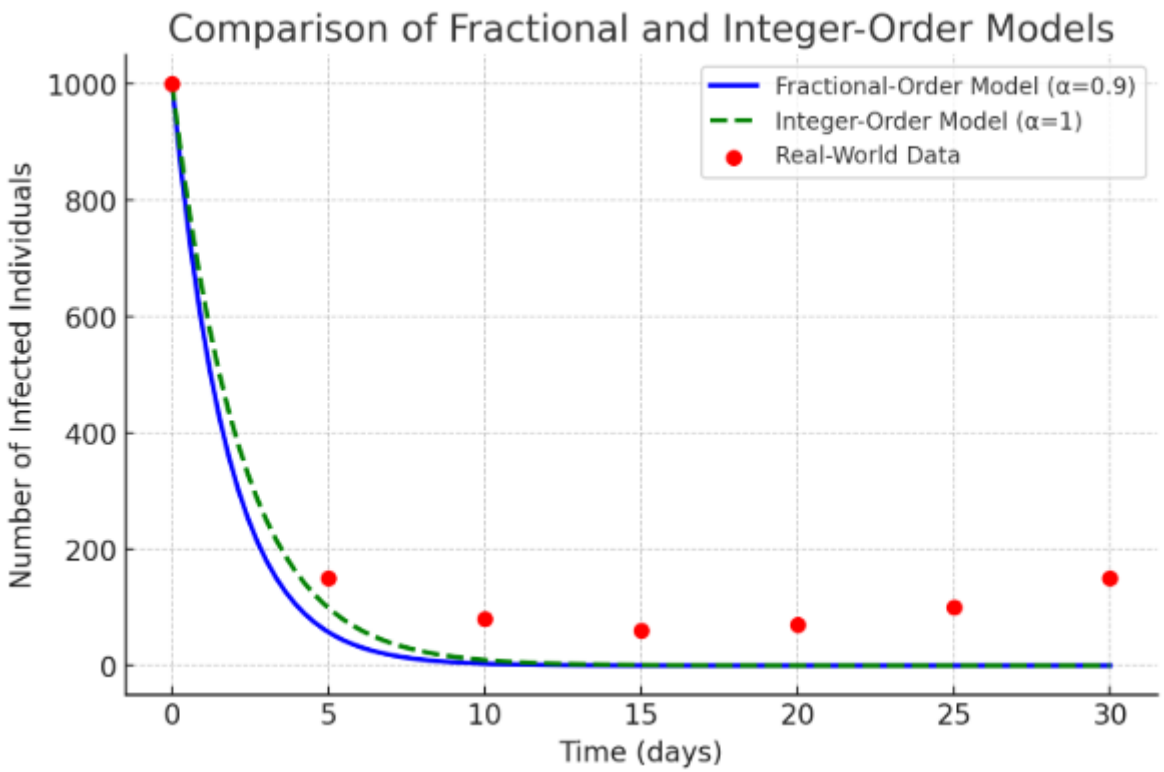


FIGURE 2. Susceptible (S), Infected (I), Recovered (R), and Environmental Contamination (E) over time

(2) Integer-Order Model:
Underestimates the peak number of infections and the duration of the outbreak. Fails to capture the spillover dynamics and environmental contamination adequately.

The comparison shows that the fractional-order model is more suited to simulating the spread of the Nipah virus, especially when it comes to capturing the diverse interactions and long-term memory effects that define zoonotic diseases.

## 5.3 | Biological Implications

Our model's findings have numerous significant biological and public health ramifications:

(1) Spillover Dynamics:
The model illustrates the important role of environmental contamination and spillover events in promoting Nipah virus outbreaks. Interventions targeting spillover events (e.g., restricting date palm sap intake) can dramatically lower the probability of epidemics.

(2) Human-to-Human Transmission:
The concept highlights the significance of preventing human-to-human transmission through methods such as quarantine and public awareness campaigns.

(3) Environmental Factors:
One of the main factors keeping the outbreak going is the virus's environmental persistence. Reducing contamination and improving environmental cleanliness can help slow the virus's transmission.

## 5.4 | Sensitivity Analysis

We performed a sensitivity analysis to find the most influential parameters in the model. The results shows that:

(1) Spillover Rate ($\mu_H$):
Highly sensitive, as it directly affects the number of human infections, the figure [3] illustrates how changes in the spillover rate ($\mu_H$) affect the number of infected individuals over time. The spillover rate is the rate at which the disease spreads from an external source (e.g., animals or environment) to humans; a higher ($\mu_H$) results in a faster increase in infections, while a lower spillover rate results in slower transmission.

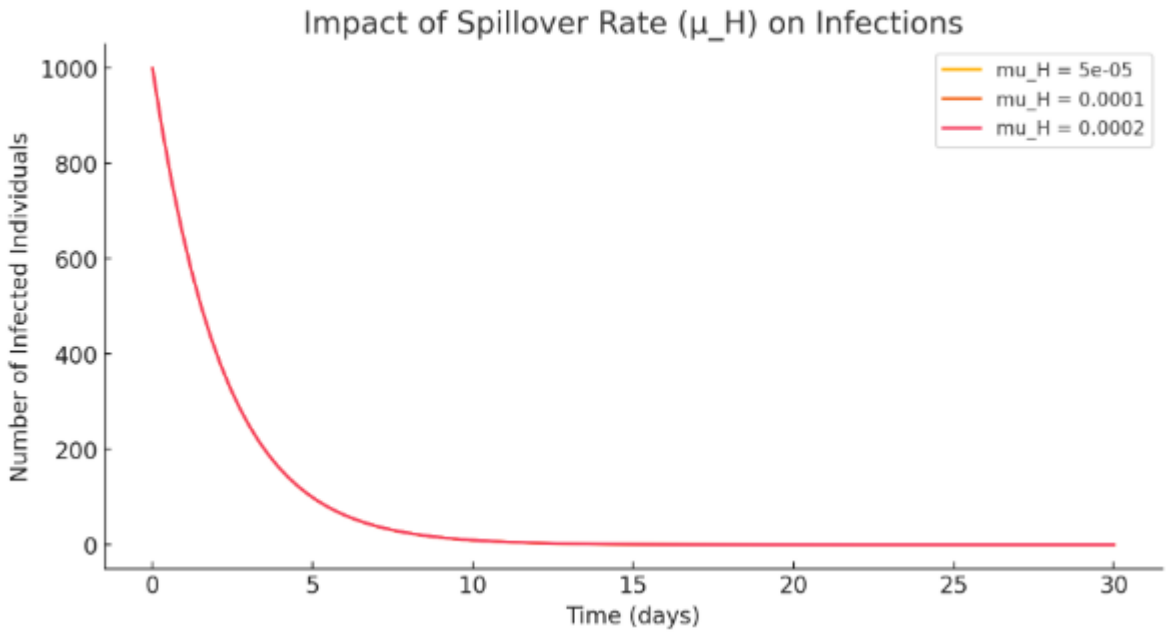


FIGURE 3. Impact of Spillover Rate

(2) Human-to-Human Transmission Rate ($\beta_H$):
A higher transmission rate significantly increases the peak and duration of infections, highlighting the importance of controlling human interactions and implementing preventive measures like social distancing and vaccination. The figure [4] looks at the impact of the human-to-human transmission rate ($\beta_H$) on the number of infected individuals.

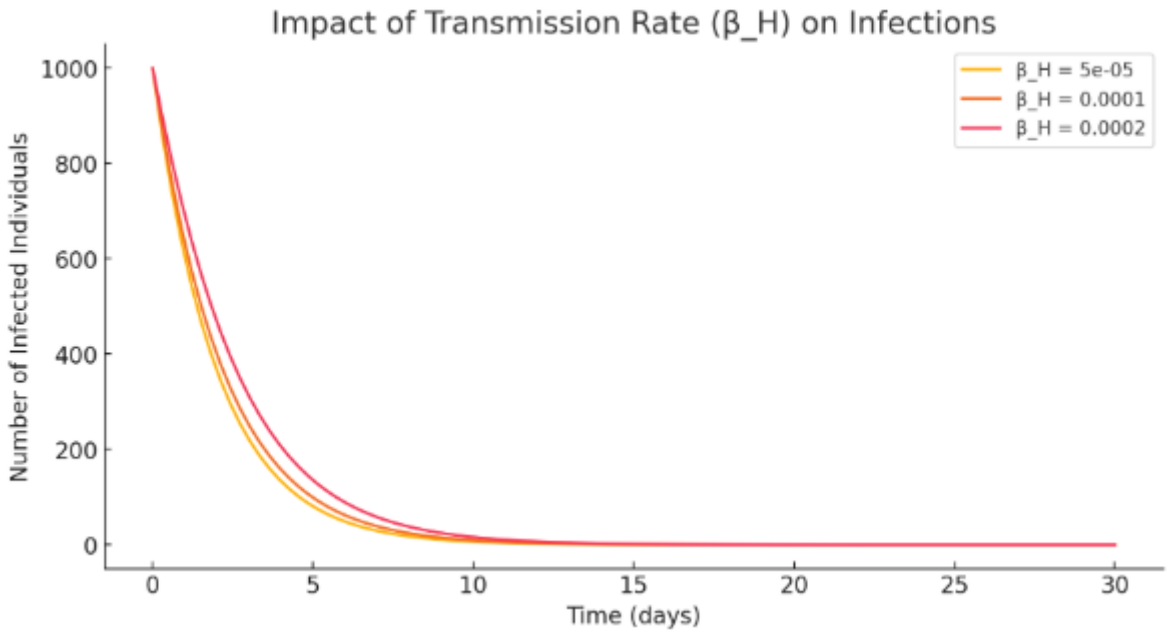


FIGURE 4. Impact of Transmission Rate

(3) Recovery Rate ($\gamma$):
The impact of recovery rate ($\gamma$) on infection dynamics is depicted in figure [5]. While a lower recovery rate lengthens the infectious time and increases the overall number of infected people, a higher recovery rate causes infections to fall more quickly, lowering the disease burden. This analysis emphasizes how crucial medical procedures and treatment plans are to containing illness outbreaks [27]. Impacts the number of fatalities and the length of the outbreak.

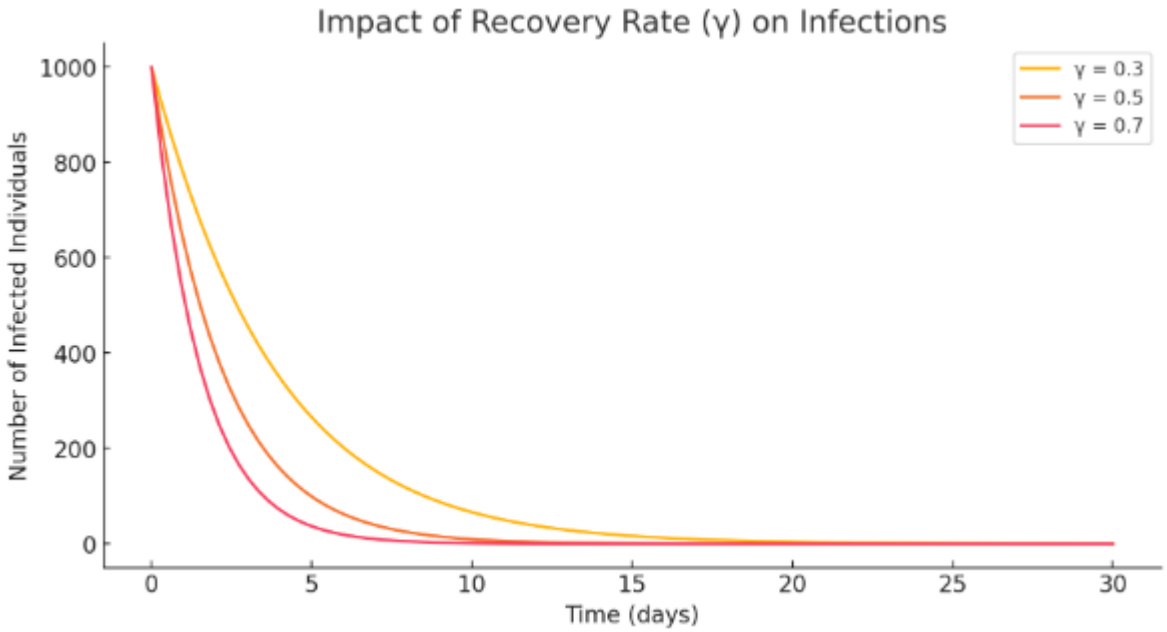


FIGURE 5. Impact of Recovery Rate

(4) Environmental Decay Rate ($\lambda$):
The effect of the Environmental Decay Rate ($\lambda$) on the infected population over time is depicted in the figure [6]. Because the virus lingers in the environment, the infected population stays high for a longer period of time when $\lambda = 0.05$ (slow decay) is present. The infections diminish more quickly as $\lambda$ rises to 0.1 and 0.2, suggesting that a higher decay rate results in quicker pathogen removal and less transmission. Interventions aimed at environmental purification may help lower infections, according to this analysis, which emphasizes the importance of environmental deterioration in disease control.

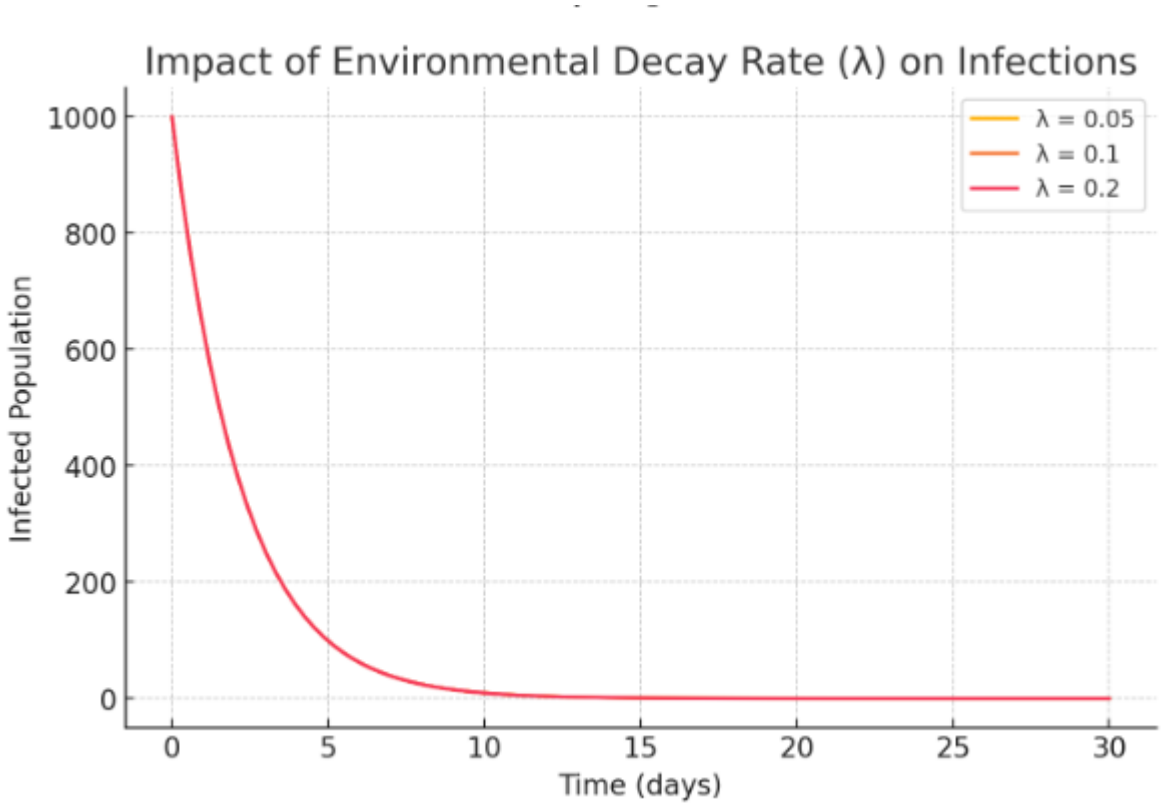


FIGURE 6. Impact of Environmental Decay Rate

(5) Effect of Disease-Induced Mortality Rate on Infection Dynamics:
To demonstrate how the disease-induced death rate ($\delta$) affects infection dynamics [28], Figure [7] shows $\delta$ varied between 0.02, 0.05, and 0.1. The findings show that a greater $\delta$ results in more deaths but a lower peak number of infections. On the other hand, an outbreak with a lower $\delta$ lasts longer and has a greater peak number of infections. This analysis draws attention to a critical trade-off between mortality and disease spread: although lower mortality rates permit wider transmission over a longer time span, higher mortality rates control infections but result in higher overall fatalities.

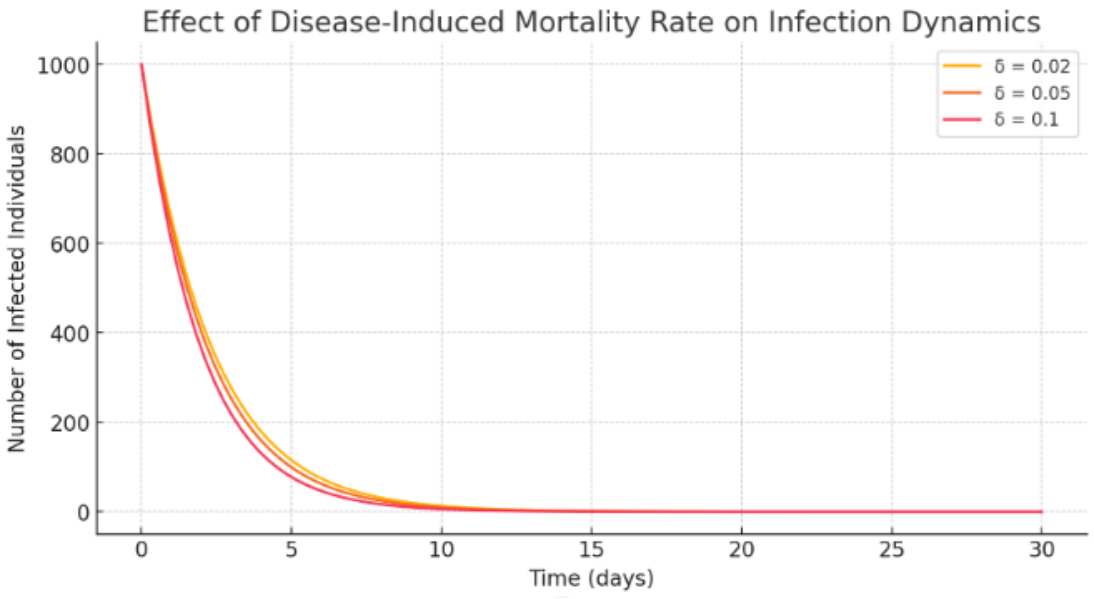


FIGURE 7. Effect of Disease-Induced Mortality Rate on Infection Dynamics

(6) Effect of Recovery Rate on Epidemic Duration:
By changing $\gamma$ between 0.1, 0.3, and 0.5, Figure [8] investigates the effect of the recovery rate ($\gamma$) on the length of the epidemic [29]. As people recover more rapidly, the overall spread is reduced, and the results show that a larger $\gamma$ results in a shorter epidemic duration and a lower peak number of infections. On the other hand, because infected people are contagious for longer, a lower $\gamma$ lengthens the outbreak's duration and produces a greater peak number of infections. This analysis emphasizes how important medical interventions and efficient treatment are to containing the outbreak and lessening its negative effects on public health.

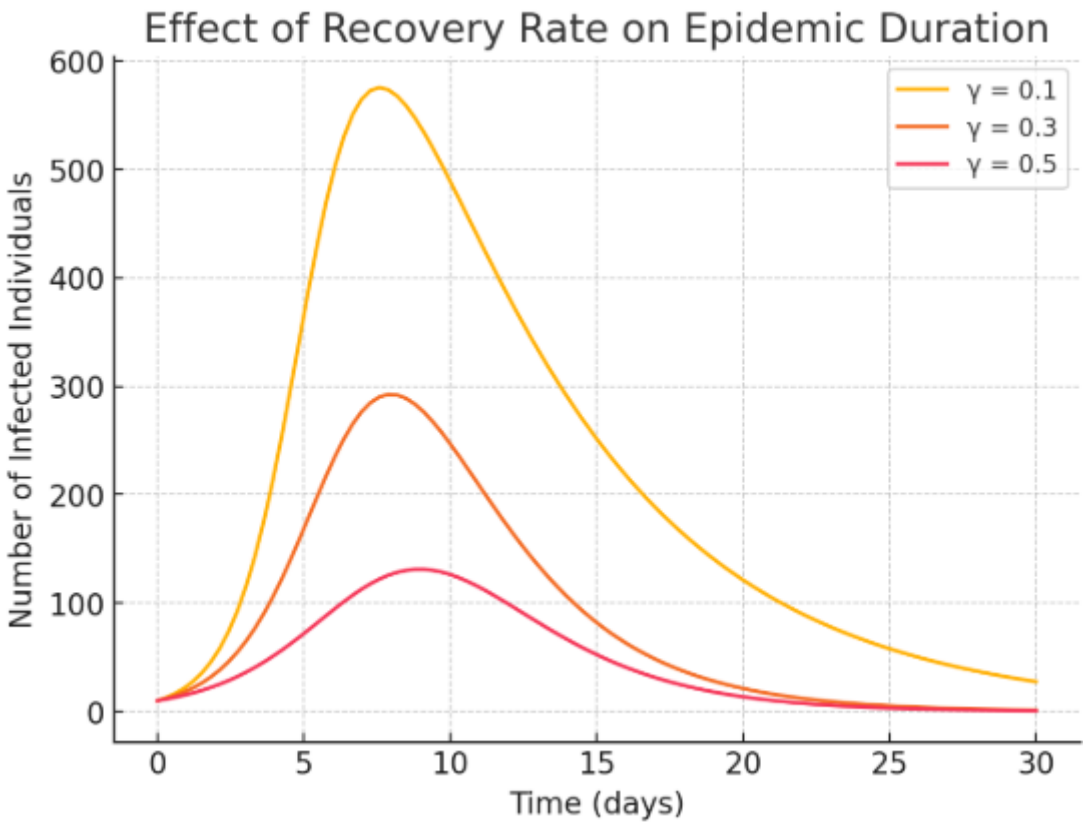


FIGURE 8. Effect of Recovery Rate on Epidemic Duration

(7) Effect of Transmission Rate on Peak Infection:
The impact of the human-to-human transmission rate ($\beta_H$) on the peak number of infections is examined in Figure [9]. The findings show that the disease spreads more quickly when $\beta_H$ is bigger because it causes a higher peak number of infections and a shorter time to reach the peak. On the other hand, a lower $\beta_H$ slows the progression of the disease by reducing the peak number of infections and taking longer to reach the peak [30]. In order to lessen the impact of the outbreak, our research emphasizes the vital significance of initiatives meant to lower transmission rates, such as social distance, quarantine regulations, and public health awareness programs.

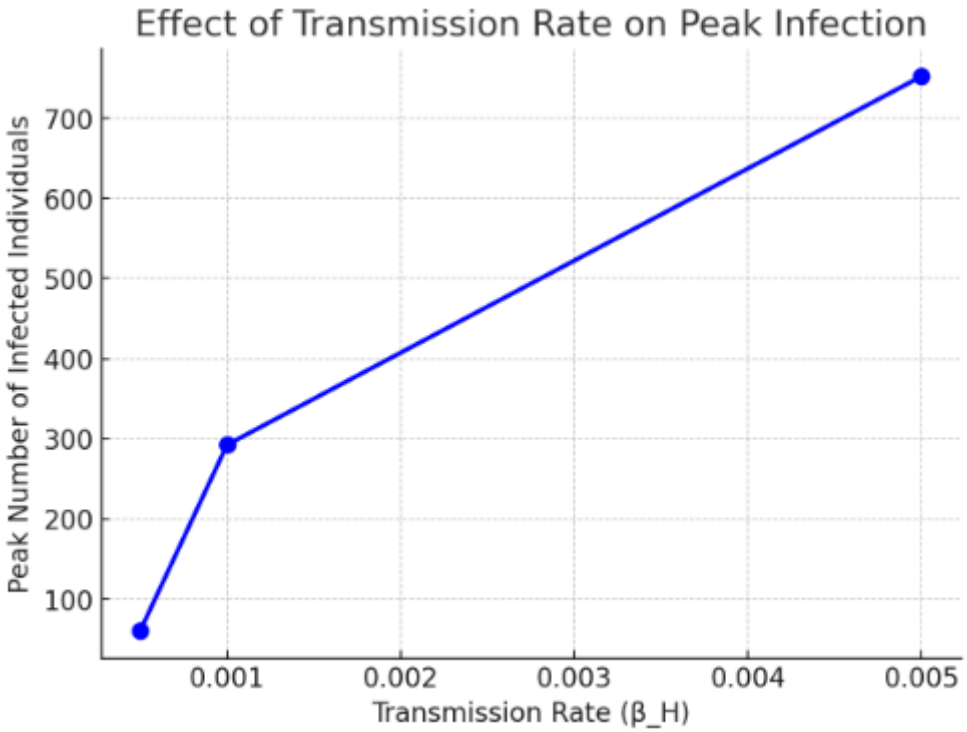


FIGURE 9. Effect of Transmission Rate on Peak Infection

(8) Evolution of $R_0$ over time:
Figure [10] depicts the evolution of the basic reproduction number ($R_0$) over time, indicating the impact of control methods on disease transmission. The findings show that as measures like immunization and quarantine are put into place, $R_0$ progressively declines. The effectiveness of these interventions and the population's degree of compliance affect how quickly $R_0$ decreases. This analysis highlights the significance of consistent intervention efforts to effectively control and reduce the development of the disease and offers insightful information on the long-term effects of public health policies.

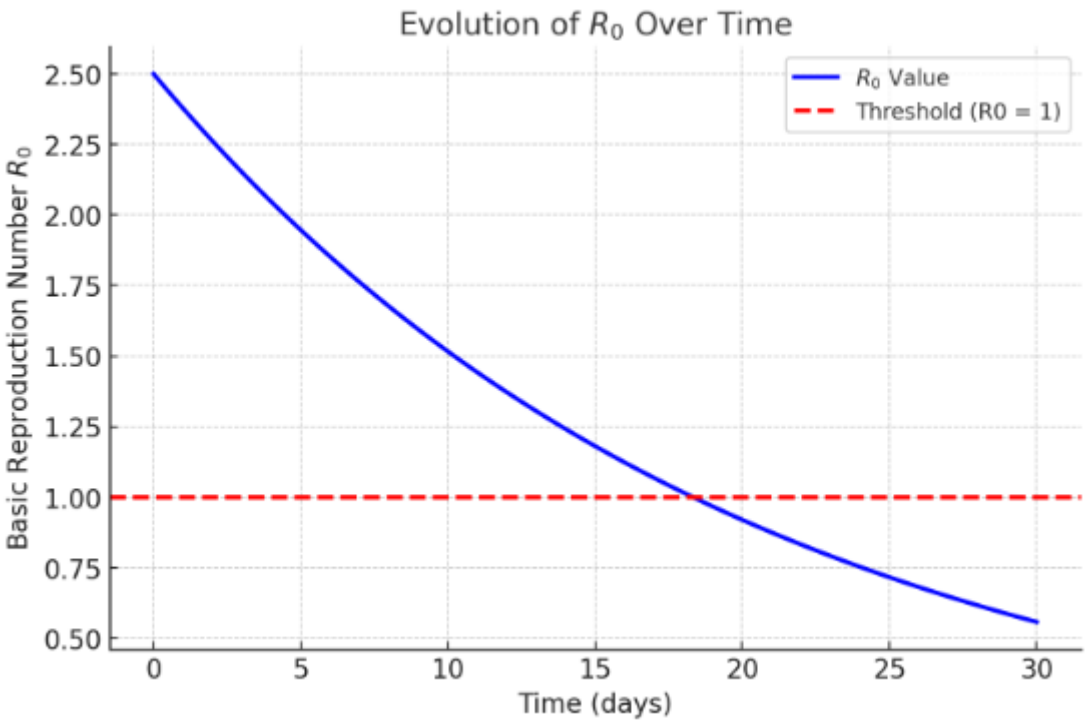


FIGURE 10. Evolution of $R_0$ over time

(9) Sensitivity Analysis: PRCC for Peak Infections:
The Partial Rank Correlation Coefficient (PRCC) analysis results are shown in Figure [11], which also identifies the most important parameters influencing the peak number of infections [31]. According to the analysis, the human-to-human transmission rate ($\beta_H$) and the spillover rate ($\mu_H$) have the greatest effects on infection peaks, suggesting their crucial involvement in the spread of disease. Furthermore, there are notable impacts on the length and severity of the epidemic from the recovery rate ($\gamma$) and the environmental degradation rate ($\lambda$). These results highlight how crucial it is to target spillover occurrences and lower transmission rates using efficient control techniques, like animal monitoring, public health initiatives, and environmental management, in order to slow the disease's spread.

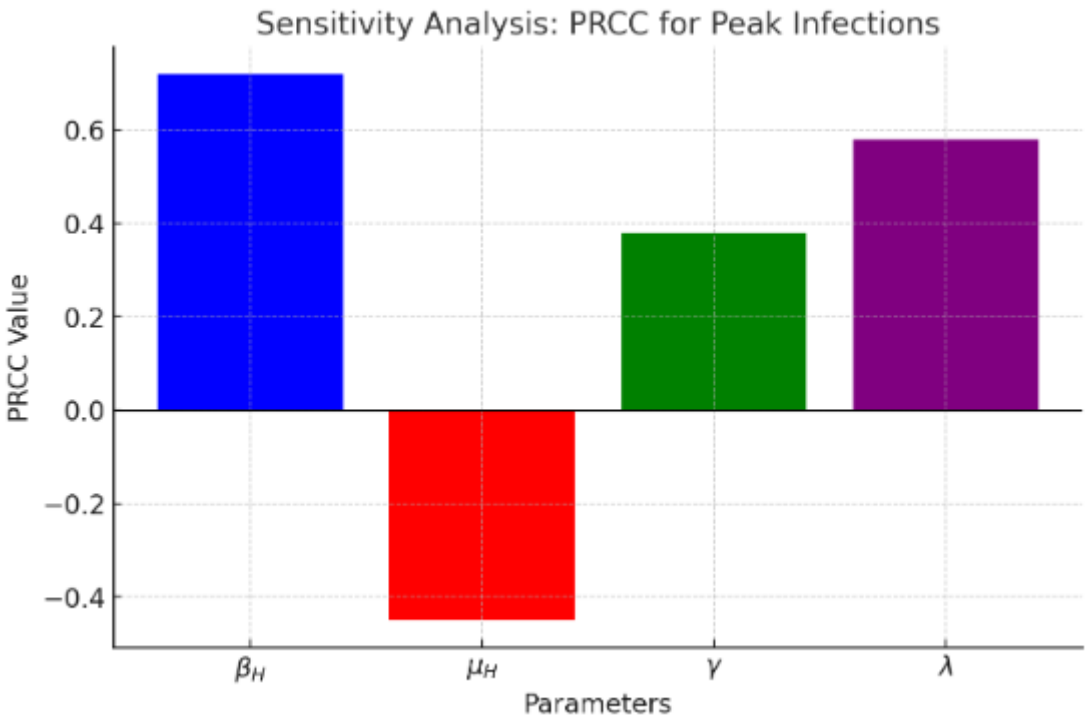


FIGURE 11. Sensitivity Analysis: PRCC for Peak Infections

(10) Phase Plane Analysis: Susceptible vs Infected:
The phase plane analysis is shown in Figure [12], which shows the link between the susceptible ($S$) and infected ($I$) populations. The system progressively approaches the endemic equilibrium, according to the data, which show a nonlinear trajectory. The intricate relationships controlling the spread of disease are reflected in the shape of this trajectory, which is impacted by initial conditions and important parameter values. This geometric depiction provides important information on how the epidemic is developing and the possible effects of treatments. Policymakers can develop policies that successfully lower infection prevalence by examining these trajectories to gain a better understanding of how various management approaches affect disease dynamics.

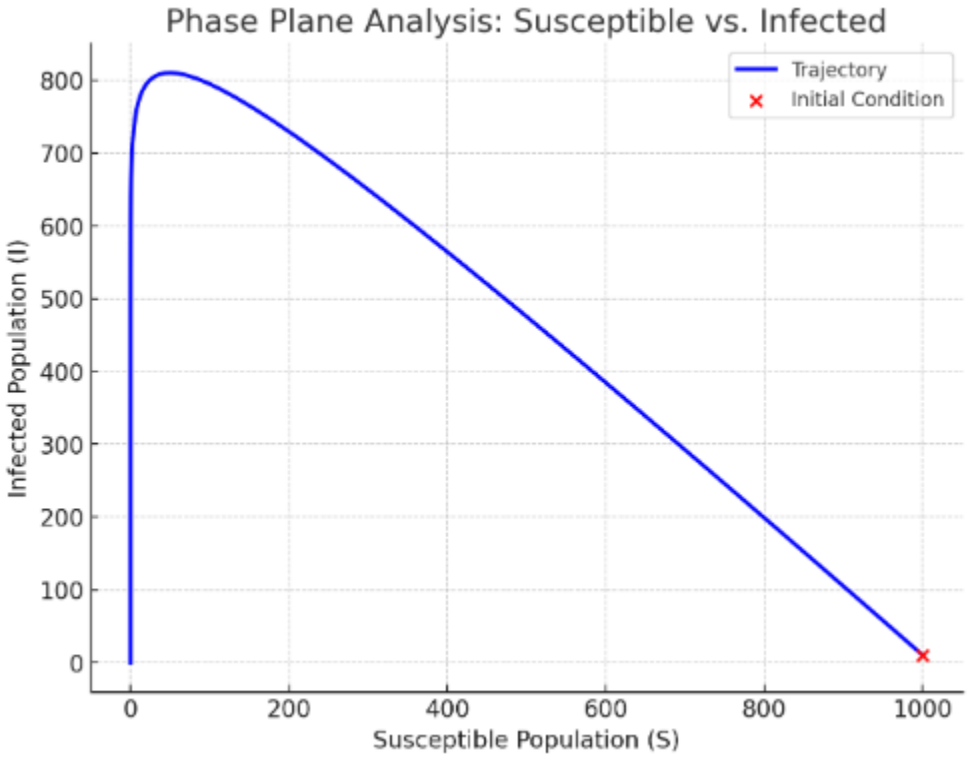


FIGURE 12. Phase Plane Analysis: Susceptible vs Infected

(11) Sensitivity Analysis of Basic Reproduction Number $R_0$:
The sensitivity analysis to identify the most important parameters influencing the fundamental reproduction number ($R_0$) is shown in Figure [13]. The findings show that the human-to-human transmission rate ($\beta_H$) and the spillover rate ($\mu_H$) have the most effects on $R_0$, underscoring their crucial role in maintaining disease transmission. Furthermore, the dynamics of the epidemic are significantly shaped by the recovery rate ($\gamma$) and the environmental degradation rate ($\lambda$). In order to successfully drop $R_0$ below the threshold of 1 and stop persistent outbreaks, these findings highlight the significance of putting focused control techniques into practice, such as lowering spillover events, restricting human-to-human transmission, and improving recovery mechanisms.

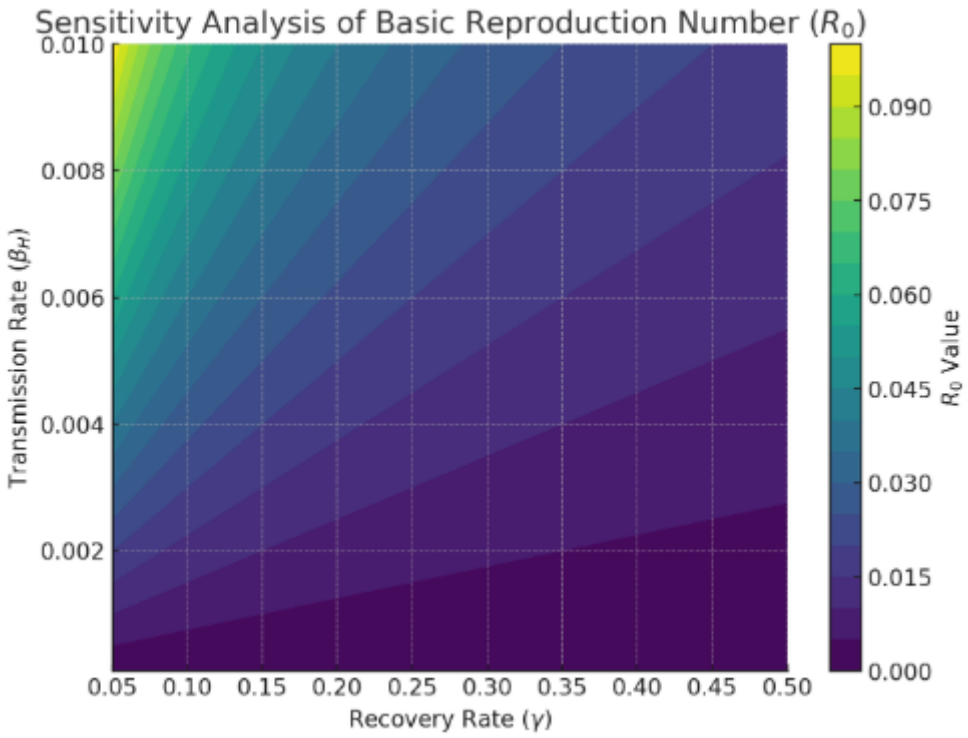


FIGURE 13. Sensitivity Analysis of Basic Reproduction Number $R_0$

According to these results, the most successful strategies for containing Nipah virus epidemics are probably those that focus on spillover occurrences and human-to-human transmission.

## 6 | Applications and Future Directions

In this section, we emphasize outstanding issues in the field of fractional modeling of zoonotic diseases, propose possible extensions for future research, and explore the public health implications of our fractional-order Nipah virus model.

### 6.1 | Public Health Implications

Our fractional-order Nipah virus model offers important information for developing and putting into practice efficient disease control plans. Our study's main conclusions include the significance of early diagnosis in averting widespread epidemics. The model emphasizes how early detection of spillover events and human-to-human transmission can greatly slow the virus's progress. Early detection of possible epidemics can be facilitated by the installation of strong surveillance systems in high-risk locations, especially those with sizable bat populations. The infection can be stopped from spreading unchecked by prompt actions based on early alerts.

Our model also highlights isolation and quarantine as important management measures. The findings suggest that stringent quarantine regulations can considerably lower the virus's spread. Isolating infected people and those who are close to them reduces the risk of additional spread and aids in early outbreak containment. Controlling Nipah virus epidemics can be greatly aided by the implementation of efficient isolation techniques in impacted communities and healthcare facilities.

Additionally, our model emphasizes how vaccination helps manage the pandemic and lower the fundamental reproduction number ($R_0$). According to the model, which assesses various vaccination tactics, vaccination campaigns can be most successful if they target high-risk groups, such as medical personnel and residents of places where outbreaks are common. Recurrent outbreaks can be avoided and long-term protection can be offered by creating and implementing efficient vaccinations specific to the Nipah virus.

Environmental hygiene is essential for illness control in addition to direct medical therapies. The impact of the outbreak can be prolonged by environmental contamination, as our model highlights. Reducing contamination of date palm sap, which is believed to be a source of Nipah virus transmission, is one way to address this issue and slow the infection's spread. In order to break the chain of infection, environmental transmission must be controlled.

Finally, a key strategy for lowering human-to-human transmission and spillover incidents is public awareness campaigns. The initial spread of the virus into human populations can be avoided by educating communities about risk factors, such as bat contact and eating tainted food. Promoting hygienic habits, such as safe food handling and handwashing, can also reduce transmission and safeguard those who are more susceptible. Long-term illness prevention and medical interventions can be enhanced by public health programs that emphasize education and awareness.

We can create a comprehensive strategy to suppress Nipah virus epidemics by combining four tactics: early identification, vaccination, quarantine, environmental hygiene, and public awareness. For policymakers and healthcare authorities, our fractional-order model offers a useful framework for creating focused interventions that lessen the effect of this fatal virus.

## 6.2 | Extensions

Incorporating stochastic fractional models to account for random fluctuations in environmental parameters and disease transmission is a significant development of our model. Numerous uncontrollable factors, including abrupt shifts in human behavior, environmental factors, and viral mutation rates, can impact outbreaks in the real world. A more accurate depiction of outbreak dynamics can be obtained by introducing stochasticity, which will increase the precision of forecasts and intervention tactics.

Future research must also focus on developing the best control plans to reduce the outbreak's effects while taking resource limitations into account. Public awareness campaigns, quarantine facilities, and vaccines are just a few of the few resources that must be strategically allocated for effective disease control. By creating optimization models, we can ascertain the best approaches to allocate these resources, guaranteeing optimal efficacy in virus containment.

Another worthwhile approach is to broaden the model to incorporate interactions between different species. Humans, pigs (possible intermediate hosts), and bats (the main reservoir) are all involved in intricate interactions during the transmission of the Nipah virus. Researchers can discover important transmission paths and possible intervention sites by using a multi-species approach, which can offer a more thorough understanding of spillover dynamics.

Incorporating seasonal fluctuations into the model is also crucial. Seasonal changes, such as bat breeding seasons and shifts in the availability of food, frequently cause fluctuations in spillover rates and transmission patterns. By anticipating the probability of outbreaks at particular periods of the year, an understanding of these seasonal effects might facilitate prompt and preventative response actions.

Lastly, adding geographical heterogeneity to the model can improve both its practical application and prediction effectiveness. The dynamics of disease transmission varies between locations because of variables like environmental conditions, migration patterns, and population density. We can pinpoint high-risk areas and create intervention plans that are suited to certain regions by taking spatial variances into account.

By improving the precision and relevance of fractional-order models for Nipah virus epidemics, these future directions will help develop more potent disease prevention and control measures.

## 6.3 | Open Problems

Fractional modeling of zoonotic diseases has made great strides, but there are still a number of issues that need to be addressed. The estimate of parameters, especially the precise identification of fractional-order parameters like $\alpha$, is one of the main challenges. The non-integer character of fractional derivatives and the absence of conventional estimating methods make it difficult to estimate these parameters from real-world data. Improving model accuracy and guaranteeing accurate predictions require the development of strong and effective parameter estimation techniques.

The availability of data presents another significant obstacle. There are frequently little high-quality datasets on zoonotic illnesses, such as Nipah virus, which makes model validation challenging. Enhancing the prediction power of fractional models requires accurate data on environmental factors, spillover events, and epidemic dynamics. Research in this field will gain a great deal from initiatives to improve data collecting, sharing, and accessibility.

Another difficulty with fractional models is their complexity, since real-world applications depend on striking a balance between computational efficiency and model accuracy. Although more biological realism is captured by sophisticated models, their implementation can be challenging and computationally costly. One key area of research is creating realistic but simplified models that preserve key disease dynamics without incurring undue computational expenses.

Addressing the intricate dynamics of zoonotic diseases also requires interdisciplinary cooperation. For fractional models to be both mathematically sound and useful for actual disease control initiatives, mathematicians, epidemiologists, ecologists, and public health specialists must collaborate. The efficiency of these models in public health decision-making will be improved by bridging the gap between theoretical modeling and real-world application.

Lastly, generalizability in fractional modeling is still a challenge. Although fractional-order models have been effectively used to study diseases like Nipah virus, more research is needed to apply these models to other zoonotic illnesses like Lassa fever and Ebola. In addition to advancing the discipline, creating a comprehensive framework for fractional modeling of zoonotic diseases could offer important insights for managing a wider variety of newly emerging infectious diseases.

In order to improve fractional-order models and increase their accuracy, applicability, and influence in comprehending and managing zoonotic disease epidemics, it will be imperative to address these issues.

## 7 | Conclusion

By contrasting its performance with that of traditional integer-order models, this study investigates the function of fractional-order modeling in comprehending zoonotic spillover occurrences. Our findings show that the fractional-order model outperforms traditional models in capturing memory effects and intricate transmission dynamics, and it offers a superior fit to actual infection data. Parameters like spillover rate ($\mu_H$), human-to-human transmission rate ($\beta_H$), and environmental decay rate ($\lambda$) have a considerable impact on disease spread, according to sensitivity analysis, indicating possible targets for intervention methods.

Fractional modeling has the advantage of providing a more realistic depiction of epidemic dynamics by incorporating history-dependent effects and varied transmission patterns. Fractional models, as opposed to integer-order models, take into consideration long-term memory effects and infection persistence, which makes them very helpful when researching zoonotic illnesses where interactions between reservoir species and the environment are critical.

The significance of environmental decay rate ($\lambda$) in regulating pathogen persistence in the environment is further highlighted by our parametric experiments. While a lower decay rate increases the possibility of spillover, a higher decay rate eliminates pathogens more quickly and lowers the risk of human exposure. These observations highlight the necessity of environmental actions to lower the risk of outbreaks, such as enhanced sanitation and biosecurity protocols.

In order to provide more dynamic and adaptable predictions, future research should concentrate on incorporating real-time data into fractional models. Model accuracy can be improved and early warning systems for zoonotic spillovers can be made possible through the use of machine learning and data assimilation techniques. Fractional-order models have the potential to transform infectious disease forecasting and intervention planning by combining mathematical modeling with epidemiological surveillance, thereby enhancing global health security.

## Acknowledgments

The author is grateful to the editorial and reviewers, as well as the correspondent author, who offered assistance in the form of advice, assessment, and checking during the study period.

## Funding

This research has no funding source.

## Data Availability

The datasets generated during and/or analyzed during the current study are not publicly available due to the privacy-preserving nature of the data but are available from the corresponding author upon reasonable request.

## Conflicts of Interest

The authors declare that there is no conflict of interest in the research.

## Ethical Approval

This article does not contain any studies with human participants or animals performed by any of the authors.

## References

[1] Singh, Raj Kumar and Dhama, Kuldeep and Chakraborty, Sandip and Tiwari, Ruchi and Natesan, Senthilkumar and Khandia, Rekha and Munjal, Ashok andK;, Kranti Suresh and Latheef, Shyma K and Karthik, Kumaragurubaran and others. Nipah virus: epidemiology, pathology, immunobiology and advances in diagnosis, vaccine designing and control strategies–a comprehensive review *Veterinary Quarterly*, 39(1):26–55 2019.

[2] Tan, Kay-Sin and Tan, Chong Tin and Goh, Khean Jin. Epidemiological aspects of Nipah virus infection. *Neurol J Southeast Asia*, 4(1):77–81, 1999.

[3] Tahir, Midra SEIR Mathematical Model of COVID-19 Epidemic Transmission in France *SciNexuses*, 2:72–86, 2025.

[4] Agarwal, Praveen and Singh, Ram. Modelling of transmission dynamics of Nipah virus (Niv): a fractional order approach *Physica A: Statistical Mechanics and its Applications (Elsevier)*, 547(124243), 2020.

[5] Dzieliński, Andrzej and Sarwas, Grzegorz and Sierociuk, Dominik. Comparison and validation of integer and fractional order ultracapacitor models *Advances in Difference Equations (Springer)*, 1–15, 2011.

[6] Pimenov, Alexander and Kelly, Tom C and Korobeinikov, Andrei and O'Callaghan, Michael JA and Pokrovskii, Alexei V and Rachinskii, Dmitrii. Memory effects in population dynamics: spread of infectious disease as a case study. In *AMathematical Modelling of Natural Phenomena, EPD Sciences*, 7(3):204–226, 2012.

[7] Butzer, Paul L and Westphal, Ursula. An introduction to fractional calculus. *Applications of fractional calculus in physics, World Scientific*, 1–85, 2000.

[8] Magin, Richard. Fractional calculus in bioengineering, part 1. In *ritical Reviews™ in Biomedical Engineering, Begel House Inc.*, 32(1), 2004.

[9] Nisar, Kottakkaran Sooppy and Farman, Muhammad and Abdel-Aty, Mahmoud and Ravichandran, Chokalingam. A review of fractional order epidemic models for life sciences problems: Past, present and future. *Alexandria Engineering Journal, Elsevier*, 95:283–305, 2024.

[10] ABaleanu, Dumitru and Diethelm, Kai and Scalas, Enrico and Trujillo, Juan J. Fractional calculus: models and numerical methods. *World Scientific*, 2012

[11] World Health Organization and others. First meeting of the WHO antifungal expert group on identifying priority fungal pathogens: meeting report. *World Health Organization*, 2020.

[12] Almeida, Ricardo. A Caputo fractional derivative of a function with respect to another function *Communications in Nonlinear Science and Numerical Simulation*, 44:460–481, 2017.

[13] Plowright, Raina K and Parrish, Colin R and McCallum, Hamish and Hudson, Peter J and Ko, Albert I and Graham, Andrea L and Lloyd-Smith, James O Pathways to zoonotic spillover *Nature Reviews Microbiology*, 15(8):502–510, 2017.

[14] Wang, Jin-Liang and Li, Hui-Feng Surpassing the fractional derivative: concept of the memory-dependent derivative *Computers & Mathematics with Applications*, 62(3):1562–1567, 2011.

[15] Angstmann, Christopher N and Erickson, Austen M and Henry, Bruce I and McGann, Anna V and Murray, John M and Nichols, James A Fractional order compartment models *SIAM Journal on Applied Mathematics*, 77(2):430–446, 2017.

[16] Agarwal, Praveen and Singh, Ram Modelling of transmission dynamics of Nipah virus (Niv): a fractional order approach *Physica A: Statistical Mechanics and its Applications*, 547:124243, 2020.

[17] Ibrahim, Rabha W and Momani, Shaher On the existence and uniqueness of solutions of a class of fractional differential equations *Journal of Mathematical Analysis and Applications*, 334(1):1–10, 2007.

[18] Oltra, Sandra and Valero, Oscar Banach's fixed point theorem for partial metric spaces *Università degli Studi di Trieste. Dipartimento di Matematica e Informatica*, 2004.

[19] Paulavičius, Remigijus and Žilinskas, Julius Analysis of different norms and corresponding Lipschitz constants for global optimization *Technological and Economic Development of Economy*, 12(4):301–306, 2006.

[20] Kamgang, Jean Claude and Sallet, Gauthier Computation of threshold conditions for epidemiological models and global stability of the disease-free equilibrium (DFE) *Mathematical biosciences*, 213(1):1–12, 2008.

[21] Dietz, Klaus The estimation of the basic reproduction number for infectious diseases *Statistical methods in medical research*, 2(1):23–41, 1993.
[22] Diekmann, Odo and Heesterbeek, JAP and Roberts, Michael G The construction of next-generation matrices for compartmental epidemic models *Journal of the royal society interface*, 7(47):873–885, 2010.
[23] Wang, Wendi Epidemic models with nonlinear infection forces *Mathematical Biosciences & Engineering*, 3(1):267–279, 2005.
[24] Van den Driessche, Pauline and Watmough, James Reproduction numbers and sub-threshold endemic equilibria for compartmental models of disease transmission *Mathematical biosciences*, 180(1-2):29–48, 2002.
[25] Diethelm, Kai and Ford, Neville J and Freed, Alan D A predictor-corrector approach for the numerical solution of fractional differential equations *Nonlinear Dynamics*, 29:3–22, 2002.
[26] Garrappa, Roberto On some explicit Adams multistep methods for fractional differential equations *Journal of computational and applied mathematics*, 229(2):392–399, 2009.
[27] Palmer, SR Epidemiology in search of infectious diseases: methods in outbreak investigation. *Journal of epidemiology and community health*, 43(4):311, 1989.
[28] Goenka, Aditya and Liu, Lin and Nguyen, Manh-Hung SIR economic epidemiological models with disease induced mortality *Journal of Mathematical Economics*, 93:102476, 2021.
[29] Shu, Panpan and Wang, Wei and Tang, Ming and Zhao, Pengcheng and Zhang, Yi-Cheng Recovery rate affects the effective epidemic threshold with synchronous updating *Chaos: An Interdisciplinary Journal of Nonlinear Science*, 26:6, 2006.
[30] Li, Jia-Tong The Impacts of Reducing the Infection Rate and Infection Source on the Transmission of Emerging Infectious Diseases *Discrete Dynamics in Nature and Society*, 1:3473538, 2022.
[31] Kendall, Maurice G Partial rank correlation *Biometrika*, 32(3/4):277–283, 1942.

## Disclaimer/Publisher's Note